Journal of Practical Information Technology

J. Practical IT, 1(6): 17-24, 2020

Research Paper

Novel optical MEMS FTIR, based on Bragg grating structure

Pejman Ghasemi [a], Mohammad Javad Sharifi [b], Kian Jafari [c]

[a] Department of Electrical Engineering, Shahid Beheshti University, Tehran, Iran
p_gasemi@sbu.ac.ir
[b] Department of Electrical Engineering, Shahid Beheshti University, Tehran, Iran
mohammadjavadsharifi@yahoo.com
[c] Department of Electrical Engineering, Shahid Beheshti University, Tehran, Iran
kian.jafari@gmail.com

Received: 10 October 2020 Revised: 19 November 2020 Accepted: 17 December 2020

Abstract

Furrier transform infrared spectroscopy (FTIR) is the key instruments in all the chemical labs for the analysis of chemical compositions in many applications such as identification of organic compounds, biochemical, food safety etc. In this paper, we introduce a new FTIR system including a new Brag-grating device, a broadband light source, integrated optical waveguides, and a photodiode. The proposed system has several advantages; the ability to randomly access to different wavelengths instead of swiping all wavelength, bandwidth adjustment, high reliability, immunity to electromagnetic noise and mechanical vibrations. The device is designed analytically at first, and then the design is confirmed utilizing numerical simulations. According to the numerical simulations, a mechanical movement of about 1 um is achieved by applying of only 5-volt electrical signal. The designed device is suitable for applications in which accidental accessibility is required instead of sweeping.

Keywords: Furrier transform infrared spectroscopy, Microelectromechanical systems, Bragg grating.

How to cite the article:
P. Ghasemi, M.J. Sharifi, K. Jafari, Novel optical MEMS FTIR, based on Bragg grating structure, J. Practical IT, 2020; 1(6): 17-24,

1. Introduction

Infrared spectroscopy is based on the absorption of infrared radiation by molecules and then evaluation of the vibrational mutations of molecules and multi-atomic ions. This method has been used as a powerful and developed method for determining the structure of molecules and measurement of chemical species. It is also used primarily for the identification of organic compounds [1], although the spectra of these compounds are usually very complex and have a large number of peaks. It can be used in these cases through comparative methods. The FTIR device is one of the most widely used devices in chemistry and biochemical experiments[2]. This device has also a very high potential for detection and identifications of polymers [3] in biological applications such as cancer cell diagnosis for both clinical and research applications [4]. It also is attractive in controlling microorganisms in the context of food safety and nutrition [5]. However, these systems often have very large dimensions and need to be connected to a computer to perform the necessary analyzes [6]. That's why they are very expensive. In recent decades, attempts to minimize the dimensions of mechanical systems using the technology of MEMS (Microelectromechanical systems) has attracted. This silicon-based technology due to the ability to achieve smaller dimensions, resulting in portability, lower cost and the possibility of integrating mechanical systems with CMOS technology are very attractive. So, efforts have been made to build MEMS-based FTIR systems. Traditional systems for spectroscopy often operate on the interferometer method. In the interferometer, a light beam is divided into two paths, and then the two light beams are re-combined and producing a pattern of interference based on superposition principle. The change in the distance of each one of the paths changes the

pattern of interference, then the detector converts this pattern to the electrical signal that can be analyzed using the computer to result in the infrared spectra of the sample. Several studies have been conducted for implementing the MEMS-FTIR device based on this method (such as Mr. Khalil et al work). They proposed a FTIR system based on the above method and the Michelson interferometer, and electrostatic parts [7]. In their research, a piece of silicon was used as the optical component for reflection, so different interference spectra are obtained by moving of the reflector| in one direction. However, the Michelson interferometer which is based on an alert mirror was very sensitive to mechanical movements [6], and any vibration can cause the output spectrum to become different. On the other hand, in order to obtain the output, it is necessary to determine the precise location of the mirror at any moment, and therefore an internal measuring system is required. Other methods that are used are based on grating, which is called lamellar grating interferometer (LGI). In these systems, two beams pass through a splitter, one to a constant grating, and another to the dynamic grating. The resulted pattern is then recorded and evaluated by a computer. Mr. Ayerden et al. developed a system based on this method [8]. However, minimizing dimensions of these systems is difficult and end to many problems. The mechanical systems in MEMS technology often has a very low range of motion, but most of the systems designed for FTIR based on the mentioned methods, due to the need to sweep a wide range of wavelengths, should have a large range of motion and need techniques such as electrostatics [7,8], or the usage of complex mechanical methods [9]. In the electrostatic method, a high voltage of about 50 volts or greater is often required to reach the high motion range.

On the other hand, the need for high speed in the sweeping of the wavelength spectrum often causes resonance in some pieces of the system and it is necessary to reduce the amplitude of the motion in the resonance frequencies by using high air pressure and or other methods. Therefore, a trade-off between the amplitude of motion in resonance frequency and the sweep speed is usually established. Resolution is one of the measurement parameters that should also be considered. High enough resolution of a measurement can effectively impact the interpreting of the measurement results, especially in complex organic compounds. Most of the target molecules are surrounded by other molecules and their measurement is difficult. The structure used for FTIR have low frequency accuracy due to the high speed. Therefore, it is necessary that the frequency pitch of sweep be very slim for more accuracy [6].

Operation principle

The Micro-Opto-Electro-Mechanical Systems *(*MOEMS*)* structure introduced in this paper is based on the movement of the photonic crystal layer. The wavelength of the output is swept by movement of the photonic crystal layer. First, a broadband source with a wavelength (0.7 to 4 micro) in the conventional optical fiber coupled to the input waveguide. The light enters the waveguide after passing through the photonic crystal. Thus reflected light is passed through a fiber to the detector. It converts the optical wave into an electrical signal. In this case, by applying electrical signals to the input pins, the output wavelength can be changed. The internal structure of the device consists of a grating structure, where each arrangement of grating can be implemented by applying a binary signal to the input pins of the device. As shown in Figure 1. The central mass of the arms is connected to the side supports by flexible foundations. These arms are connected from one side to the each other, which is called a common electrode, and on the other side, each of them is attached separately to the pads. So that the electrical signal can be applied to they through the input pins. By applying the electrical voltage to each of the inputs in the arm relative to that base, the electrical current causes heat generation due to the electrical resistance. Generated heat due to the effects of thermal expansion, increases the size of the arm of the brags, so there are starting to bend. In the bottom side of each brag is a few defects that forces the brags to move in the opposite direction. It also increases the range of movement of each structure. The movement of the arms causes the brags to enter or leave the optical path of the waveguide. Therefore, effective thickness of the brags changes in the optical path. As a result, the refracted optical wavelength changes in the brag structure, and any arbitrary wavelength can be removed from the input wave selectively. This structure allows us to set the frequency sweep stairs in the device as the desired. So, we can pass some wavelengths with larger steps or, conversely, at impressive wavelengths, the resolution can be increased. In other words, at a certain wavelength, do the zoom. Most of the structures that have been fabricated so far, based on interference Theory, require a very high motion range to sweep the full wavelength output. On the other hand, in linear displacement, the precise location of the mirror or reflective structure must be specified to determine the amount of output wavelength to be transmitted by this method. But in the proposed binary structure, without the use of any additional external measuring structure, it is possible to easily determine the transmission wavelength by applying electrical signals to the input pads.

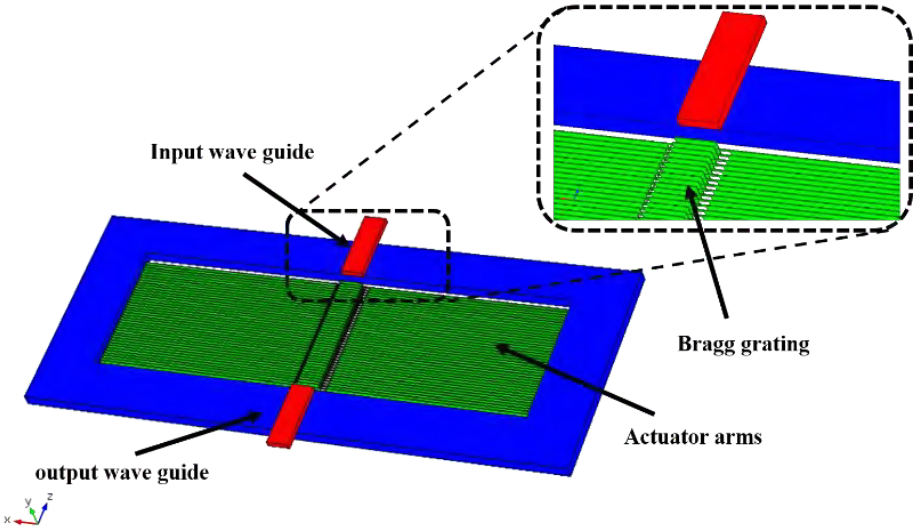

Figure 1: schematic of proposed MOEMS FTIR

In addition, the provided structures, such as [7], require very high precision DAC (Digital to Analog Converter) to convert exterior signals from the processor to analog signals for actuation, and the precision of this DAC specifies the wavelength sweep accuracy and, consequently, the resolution of the device. In addition, the device is not immune to electrical and thermal noise such as white noise, and any temperature change or electromagnetic induction causes longitudinal changes in the mirror location and eliminates the output result. For this purpose, it is often necessary to have a more complicated and costly package structure [9] and there should also be a more complex BIST (Built-in self-test) and BISC (Built-inSelf-Calibration) structure on the device. Each of it increases the cost of fabrication. While the introduced structure due to the binary nature is compatible with digital component so, there is no need for complex DAC components on it. (Figure 2).

Design and analysis of mechanical structure

Thermal response time is a key design factor in determining how quickly the MEMS device responds, especially when driven by an AC (Alternative Current) signal. From heat exchange and transfer theory, there are three mechanisms of heat flow: conduction, convection and radiation. As mentioned earlier, a beam structure has been used to thermal actuation the brags. In this scheme, the electrical current is applied through the two electrodes to the brag structure indicated in the schematic. By passing the electric current due to the electrical resistance of the arms, the heat is generated in it. The temperature increased in the arms due to this current can be calculated as follows [10]:

$$\frac{\partial T(x)}{\partial t} = \frac{k_{arm}}{C_{arm}\rho}\frac{\partial T^2}{\partial x^2} - \frac{k_{gap}P}{2C_{arm}\rho Ah}\Delta T + \frac{V^2}{RC_{arm}\rho AL} \quad (1)$$

$$T_m = \frac{2V^2h}{Rk_{arm}PL} + T_{ext} \quad (2)$$

Where T is the beam temperature, ΔT is the the temperature difference with the environment, A is the beam cross section area, P is beam cross section perimeter, V is the voltage, R is the electrical resistivity, L is the length of beam, h is the gap between the beam and the substrate, ρ is density of material, $k_{gap}$is the thermal conductivity of surrounding media, k_{arm} is the thermal conductivity of beam, C_{arm} is the heat capacity of structure, T_m is the maximum temperature of the structure

∂T^2 by neglecting of $\overline{\partial x^2}$. The structure of each brag can be mechanically modeled simply by a bending beam like a figure 2.

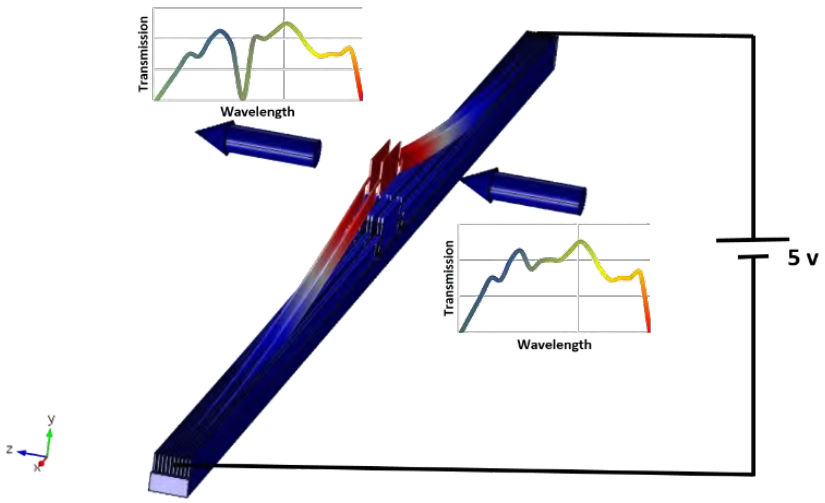

Figure 2: schematic of operation principle

The maximum deflection of the V-shape beam depends on the longitudinal dimensions and the thickness of the beam. The displacement rate can also be directly related to the amount of force involved. The temperature that is generated causing the thermal expansion in beam structure so that the V-shape beam start to bend in along the y-axis (Figure 3). The maximum displacement in V-shape beam in absent of external force is obtained using the following equation [11]:

$$y = \alpha \Delta T l \frac{\sin\theta}{\sin\theta^2 + \frac{12 I \cos\theta^2}{A l^2}} \quad (3)$$

Where, y is the maximum deflection in the middle point of beam, α is the coefficient of thermal expansion, l is the beam length, A is the beam cross section, I is the moment of inertia.

Numerical analysis of mechanical structure

The maximum displacement in y-axis direction and temperature of V-shape beam can numerically analyzed by Comsol multi-physics. the results obtained with this parameters [12-14]: The arm material is polysilicon with 80 um long, 100 nm wide, 1 um height and 2 um gap, with angle θ = 10, Young modulus, E = 152.9 GPa, Poisson ratio, ν = 0.2, resistivity $\rho = 3.74 \times 10^{-4}$ ($\Omega. m$), thermal expansion coefficient, $\alpha = 2.6 \times 10^{-6}$ (K^{-1}) , density, 2320 (kgm^{-3}) , thermal conductivity, k_{arm} = 34 ($kWm^{-1}K^{-1}$), $k_{gap} = 0.05$ ($Wm^{-1}K^{-1}$). For modeling, the finite element analysis (FEA) of the coupled Joule heating and solid mechanic are used to deriving displacement and force. In this study, it is assumed that the thermal expansion coefficient varies with temperature. It is also assumed that thermal actuators are surrounded with air media and the temperature transmission is carried out with the body. However, the thermal expansion in the body is neglected. The heat generated by joule heating is considered to be a thermal equilibrium and is distributed uniformly throughout the surface of the piece. The temperature in the anchor's location due to the connection to the body and due to the temperature losses is assumed to be in equilibrium with the surrounding environment then it's set at room temperature 25℃ as a boundary condition. Polysilicon is chosen as a body material of thermal actuators, which is considered uniform in the simulation. The FEA results show that in the maximum displacement 1um (Figure 4). The maximum temperature also is 440 ℃ , this temperature is much less than of the melting point of polysilicon. This temperature was generated by voltage about 5 v.

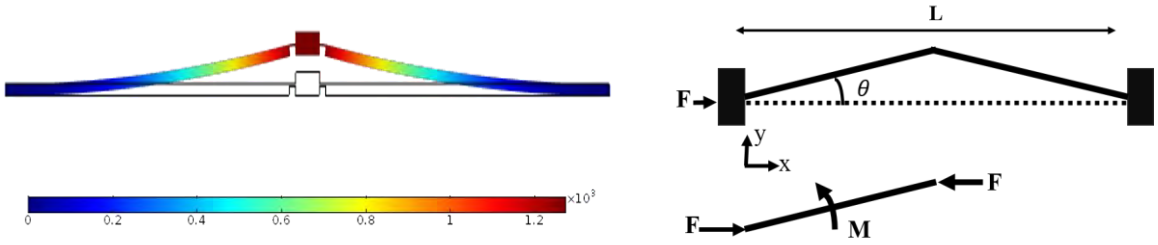

Figure 3: mechanical simulated of device.

Design and analysis of optical sensing system

The optical system is an important part of the FTIR structure. This system should choose a specific wavelength of light to pass and other wavelengths will not pass. This system is as shown in the figure [2]. A photonic crystal consists of several consecutive layers known as gratings. By applying an electrical signal to anchors in this structure, the brags are moved so that, the effective grating length has been changed. The Bragg grating structure acts based on Fresnel law, the return wavelength, known as the wavelength of the Bragg, is calculated according to the equation below[15]:

$$\lambda=2n\Lambda \quad (4)$$

Where *n* is the reflection index, Λ is the bragg period, λ is the reflaction wavelength. In Figure. 5 reflectance spectra of the photonic crystal of the proposed filter is shown for five different applied voltages. If the movable arms are initially positioned without external stimulation the reflected wavelength all will pass. Any selection of the wavelength is caused by external stimulation. By stimulating the anchors with a particular arrangement, the arms move in the direction that the brags are allocated in the optical path. The placement of the brags in the optical path causes the wavelength to be reflected in proportion to it, and the rest of the wavelengths pass. By changing the order of stimulation to the anchors, another arrangement of brags can be created in the optical pathway that changes the reflected wavelength so that different wavelengths can be selected with sequential or random access. Therefore, this system in addition to the FTIR applications, can be used in more diverse applications, such as multiplexers[16] or optical filters [16-18]. Using random access to different brags ordination allows us to achieve special properties that cannot be implemented through conventional optical structures. In general, there are several parameters that can affect the optical properties of a Brag grating such as brag wavelength and grating strength [19] . There are also properties that it is better to have the controlling of them, depending on the desired, such as transmission power and bandwidth. The reflection power related to the effective length of the brags [20]. Further lengths have higher reflection power. This possibility is provided for the system with random access that can control the amount of power through increasing or decreasing the Bragg length, so by applying the arrangement of Braggs in the optical path, it let to pass less or more of the transmission power to the output. On the other hand, since the grating strength is related to the bandwidth[19], so by controlling of it can control bandwidth. In these methods, as shown in Figure 6, by applying a special arrangement of Braggs in the optical path can be controlled bandwidth to increase or decrease. In this structure, by inducing the Braggs in the optical path, the thickness of the layer with a higher refractive index can be more or less than the intended length for the air gap, or vice versa. Notice that it is necessary that the overall period of the Bragg is fixed to obtain a central frequency, but unlike the conventional method, which determines the thickness of each component of the Bragg in terms of refractive index, in this case the contribution of one or both of the components of the Bragg structure increases or decreases. Therefore, according to Figure 6, the possibility of changing in bandwidth and zoom in wavelength can be made. Therefore, for rapid changes in bandwidth, the thickness of both Braggs increases or decreases, but if the objective is to reduce the bandwidth gradually, it can be made by changing only one of the thicknesses, and then change the second. by this way, the change in the output bandwidth done more precisely, in other words, the output bandwidth changes in a half step. In addition to the features that can be found in the uniform structure that is known as a constant grating period. this device can use to access other features that are not available in the uniform structure [21]. For example, the possibility of creating different Bragg arrangement allows us to apply nonperiodic gratifications like chirps that have special applications and properties [22]. in this structure, the grating pitches change with a linear profile along the optical path. This allows different resonant frequencies to be created during grating [23]. by this way, if changes in gratings be

small, thus changes can be considered uniform; so, each partition of grating independently returns a different wavelength so, the reflected bandwidth can be wider.

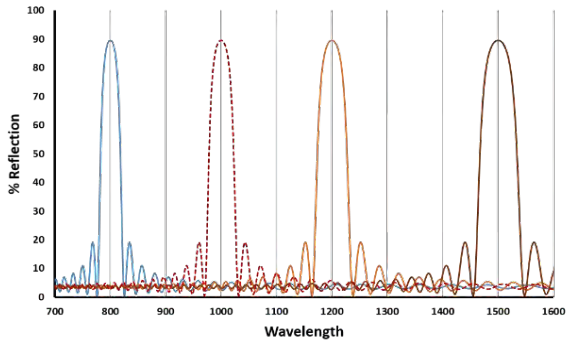

Figure 4: Reflection spectrum for the different arrangement of Braggs in the optical pathway.

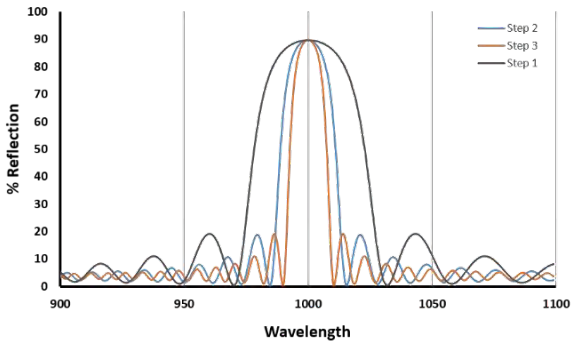

Figure 5: Reflection spectrum for non uniform Bragg thickness.

Design and analysis of stimulation system

In this system, the smaller size of the fingers, can provide us smaller sweeping steps, for example in a Bragg grating structure with a 100 nm fingernail length for a 25 um grating length. we need 250 fingers. Each of these fingers need to be driven through a circuit, which will require to have at least 250 entries per piece, which is not possible. The problem can be overcome by division Braggs in smaller units then determining a maximum wavelength and a minimum wavelength for each unit. Therefore, using a digital combinational circuit can drive any small unit. Because the arms are made from polysilicon, its compatible with CMOS process. This compatibility allows us to integrate CMOS circuits with MOEMS structure. So, according to the figure 6. Each small unit connects to a logic circuit, and the parallel circuits is driven by a driver circuit. Therefore, by applying a digital signal to input pins of the chip, the signals which needed to drive the actuators by a suitable pattern, can be reached.

Comparison study and discussion

In terms of complexity and operation condition, available systems for access to a wider range of wavelengths require high voltage operation. This high voltage, as already mentioned, is due to the electrostatic method, requires high voltage circuits. In spite of, these systems need to have feedback from their reflector position because the system is based on diffraction so that the precision determining of the reflector position due to the analogical nature of it, is critical. Therefore, they require accurate DAC and ADC circuits. This mechanism makes the system more complex, while the proposed system acts as an open loop and does not require any feedback. Furthermore, its operating voltage is about 5 volts, which is proportional to the digital system. In addition to previous challenges, these systems require different external lenses and mirrors to maintain its function, which makes the system more expensive and more sensitive to mechanical vibrations and noises. Additionally, the use of high air pressure inside the device to damp the resonance amplitude, makes the device packaging more complex, while the proposed system acts between two upper or lower levels, so mechanical noise such as vibration is not affected on it. In terms of fabrication, the proposed device is harder to fabricate due to smaller feature sizes of device components. contrary to the [13] that feature sizes are larger.

Conclusion and perspectives

In this work, an optical MEMS FTIR is proposed. The present structure operates based on the grating properties. In this device, using joule heating, the movable Braggs are placed on the optical pathway and cause a change in the optical properties of the system that achieves different wavelengths. By sweeping the wavelength and recording the optical power output, a power spectrum can be obtained. The system of wavelength sweeper includes an air-dielectric movable Bragg grating structure, a broad band light source, a photo-detector, and integrated optical waveguides. The behavior of both the mechanical actuator structure in presence of joule heating and the optical system has been studied by FEA simulations. The main features of this device include immunity to electromagnetic noise and mechanical vibrations, the ability to randomly access to different wavelengths, bandwidth adjustment, high reliability and Compatibility with digital circuits. In addition to FTIR applications, this device can be used in various applications

such as optical sensors, optical filters, frequency multiplexer in optical telecommunication networks, in the single frequency light source, and optical modulators. Fabrication of the proposed MOEMS FTIR by using Nano lithography and Deep Reactive Ion Etching (DRIE) is an ongoing work which can be the subject of a wholly different paper.

References

[1] F. Huth, A. Govyadinov, S. Amarie, W. Nuansing, F. Keilmann, and R. Hillenbrand, "Nano-FTIR absorption spectroscopy of molecular fingerprints at 20 nm spatial resolution," *Nano Lett.*, vol. 12, no. 8, pp. 3973–3978, 2012.

[2] D. Y. Duygu, T. Baykal, Đ. Açikgöz, and K. Yildiz, "REVIEW Fourier Transform Infrared (FT-IR) Spectroscopy for Biological Fourier Transform Infrared (FT-IR) Spectroscopy for Biological Studies," vol. 22, no. January 2009, pp. 117–121, 2015.

[3] J. J. Sahlin and N. A. Peppas, "Near-field FTIR Imaging : A Technique for Enhancing Spatial Resolution in FTIR Microscopy," *J. Appl. Polym. Sci.*, pp. 103–110, 1997.

[4] A. C. S. Talari, M. A. G. Martinez, Z. Movasaghi, S. Rehman, and I. U. Rehman, "Advances in Fourier transform infrared (FTIR) spectroscopy of biological tissues," *Appl. Spectrosc. Rev.*, vol. 52, no. 5, pp. 456–506, 2017.

[5] J. H. Qu *et al.*, "Applications of Near-infrared Spectroscopy in Food Safety Evaluation and Control: A Review of Recent Research Advances," *Crit. Rev. Food Sci. Nutr.*, vol. 55, no. 13, pp. 1939–1954, 2015.

[6] T. Sandner, A. Kenda, C. Drabe, H. Schenk, and W. Scherf, "Miniaturized FTIR-spectrometer based on optical MEMS translatory actuator," vol. 6466, p. 646602, 2007.

[7] D. Khalil, Y. Sabry, H. Omran, M. Medhat, A. Hafez, and B. Saadany, "Characterization of MEMS FTIR spectrometer," vol. 7930, p. 79300J, 2011.

[8] N. Pelin Ayerden *et al.*, "High-speed broadband FTIR system using MEMS," *Appl. Opt.*, vol. 53, no. 31, p. 7267, 2014.

[9] Y. S. Yang, Y. H. Lin, Y. C. Hu, and C. H. Liu, "A large-displacement thermal actuator designed for MEMS pitch-tunable grating," *J. Micromechanics Microengineering*, vol. 19, no. 1, 2009.

[10] stephan warnat and T. H. Bruno Barazani, "Simulation and Optical Measurement of MEMS Thermal Actuator Sub-micron Displacements in Air and Water," 2015, vol. 9521, pp. 3–8.

[11] Y. Zhu, A. Corigliano, and H. D. Espinosa, "A thermal actuator for nanoscale in situ microscopy testing: Design and characterization," *J. Micromechanics Microengineering*, vol. 16, no. 2, pp. 242–253, 2006.

[12] Y. Bourezig, B. Bouabdallah, and F. Gaffiot, "Analysis of the resistivity in polysilicon thin film transistors study of film thickness effect," *Istanbul Univ. - J. Electr. Electron. Eng.*, vol. 8, no. 2, pp. 733–738, 2008.

[13] H. Liu and L. Wang, "Measurements of thermal conductivity and the coefficient of thermal expansion for polysilicon thin films by using double-clamped beams," *J. Micromechanics Microengineering Accept.*, vol. 28, no. 1, p. 15010, 2018.

[14] M. S. Suen, J. C. Hsieh, K. C. Liu, and D. T. W. Lin, "Optimal design of the electrothermal V-beam microactuator based on GA for stress concentration analysis," *IMECS 2011 - Int. MultiConference Eng. Comput. Sci. 2011*, vol. 2, pp. 1264–1268, 2011.

[15] J. L. Arce-Diego, R. López-Ruisánchez, J. M. López-Higuera, and M. A. Muriel, "Fiber Bragg grating as an optical filter tuned by a magnetic field," *Opt. Lett.*, vol. 22, no. 9, p. 603, 1997.

[16] C.-C. Chiang and C.-C. Tseng, "Characterization of notched long-period fiber gratings: effects of periods, cladding thicknesses, and etching depths," *Appl. Opt.*, vol. 53, no. 20, p. 4398, 2014.

[17] C. Alonso-Ramos *et al.*, "Long-period suspended silicon Bragg grating filter for hybrid near-and mid-infrared operation," *arXiv: 1610.04917*, pp. 1–5, 2016.

[18] K. Kalli *et al.*, "Electrically tunable Bragg gratings in single-mode polymer optical fiber," *Opt. Lett.*, vol. 32, no. 3, pp. 214–216, 2007.

[19] S. Pawar, S. Kumbhaj, P. Sen, and P. K. Sen, "Fiber Bragg Grating Filter for Optical Communication : Applications and Overview," *Int. J. Adv. Electr. Electron. Eng.*, pp. 51–58, 2013.

[20] K. O. Hill and G. Meltz, "Fiber Bragg Grating Technology Fundamentals and Overview," *J. Light. Technol.*, vol. 15, no. 8, pp. 1263–1276, 1997.

[21] J. Canning and M. G. Sceats, "π-phase-shifted periodic distributed structures in optical fibres by UV postprocessing," *Electron. Lett.*, vol. 30, no. 16, pp. 1344–1345, 1994.

[22] S. Sengupta and S. K. Ghorai, "High Performance Optical Comb Filter using Full duty cycle based Periodically Chirped- Sampled Fiber Bragg Grating," no. 3, pp. 3–4, 2015.

[23] C. A. F. Marques, P. Antunes, P. Mergo, D. J. Webb, and P. Andre, "Chirped Bragg Gratings in PMMA StepIndex Polymer Optical Fiber," *IEEE Photonics Technol. Lett.*, vol. 29, no. 6, pp. 500–503, 2017.